

Mitigating Intra-Cell Pilot Contamination in Massive MIMO: A Rate Splitting Approach

Anup Mishra, Yijie Mao, *Member, IEEE*, Christo Kurisummoottil Thomas, *Member, IEEE*, Luca Sanguinetti, *Senior Member, IEEE* and Bruno Clerckx, *Fellow, IEEE*

Abstract

Massive MIMO (MaMIMO) has become an integral part of the 5G standard, and is envisioned to be further developed in beyond 5G networks. With a massive number of antennas at the base station (BS), MaMIMO is best equipped to cater prominent use cases of B5G networks such as enhanced mobile broadband (eMBB), ultra-reliable low-latency communications (URLLC) and massive machine-type communications (mMTC) or combinations thereof. However, one of the critical challenges to this pursuit is the sporadic access behaviour of the massive number of devices in practical networks that inevitably leads to the conspicuous pilot contamination problem. Conventional linearly precoded physical layer strategies employed for downlink transmission in time division duplex (TDD) MaMIMO would incur a noticeable spectral efficiency (SE) loss in the presence of this pilot contamination. In this paper, we aim to integrate a robust multiple access and interference management strategy named rate-splitting multiple access (RSMA) with TDD MaMIMO for downlink transmission and investigate its SE performance. We propose a novel downlink transmission framework of RSMA in TDD MaMIMO, devise a precoder design strategy and power allocation schemes to maximize different network utility functions. Numerical results reveal that RSMA is significantly more robust to pilot contamination and always achieves a SE performance that is equal to or better than the conventional linearly precoded MaMIMO transmission strategy.

Index Terms

Rate-splitting multiple access (RSMA), massive MIMO, pilot contamination.

I. INTRODUCTION

Massive multiple-input multiple-output (MaMIMO) has been widely regarded as one of the key technologies in 5G communication [2], [3]. With a large array of service antennas at the base station (BS), MaMIMO is capable of enhancing the spectral efficiency (SE), energy efficiency (EE) and robustness of multi-user MIMO networks [4]–[6]. A MaMIMO network can operate in both time-division duplex (TDD) and frequency-division duplex (FDD) modes. Due to the massive number of antennas, downlink

(DL) channel state information (CSI) acquisition in the FDD mode incurs a huge training overhead [7] thereby decreasing the SE of the network. In contrast, by exploiting the reciprocity of the uplink (UL) and DL physical propagation channels, CSI acquisition is much simpler in the TDD mode. At the BS, the CSI is acquired through UL training and then utilized for DL transmission [8]. As a result, the training length is proportional to the number of user equipments (UEs) rather than the number of BS antennas, which significantly reduces the CSI overhead. This makes TDD the preferred mode of operation in MaMIMO networks [7]. Even with a low CSI overhead, a TDD MaMIMO network is not without its limitations. In the UL, the CSI acquisition is preferably done by assigning orthogonal pilots to different UEs. However, due to the scarcity of orthogonal sequences, UEs are typically forced to use the same pilot for UL training, leading to the issue of pilot contamination [8], [9]. With the advent of 5G and expanded use cases in dense crowded scenarios and massive machine type communications (mMTC), the problem of pilot contamination gets further exacerbated. Within a cell, a massive number of UEs and their sporadic access behaviour make allocation of orthogonal pilots to all UEs or orthogonal scheduling of all UEs for transmission infeasible [10]–[13]. For such scenarios, random access techniques are typically employed to serve the active UEs in the network, where active UEs randomly select a pilot sequence from a small pool of orthogonal sequences for UL training. As a result, it is highly likely that multiple UEs may share the same pilot for UL training resulting in even severe *intra-cell* pilot contamination [11], [13].

The problem of pilot contamination is a major challenge in TDD MaMIMO and could lead to a significant SE loss. In fact, with uncorrelated Rayleigh fading channels, pilot contamination is known to be performance limiting [8]. To address the challenge, pilot contamination and its mitigation has been studied by a wide body of existing literature [14]–[19]. To that end, [2], [3] have proved that with spatially correlated channels and minimum mean-square error (MMSE) processing, the capacity of a MaMIMO network is asymptotically (with respect to the number of transmit antennas) unlimited despite pilot contamination. Nevertheless, the SE of a TDD MaMIMO network is practically limited and with a finite number of antennas, incurs a considerable performance loss in the presence of pilot contamination [2]. The undesired consequence of pilot contamination, i.e, low quality statistically dependent channel estimates, is well documented in the literature [8]. Designing precoders based on such low quality CSI will result in severe multi-user interference in the DL and the network may become interference limited.

One possible solution to deal with the DL multi-user interference that stems from the intra-cell pilot contamination would be to adopt the interference management strategy introduced in [20] and named rate-splitting multiple access (RSMA). RSMA has emerged as a robust physical (PHY)-layer transmission strategy and is considered as a promising paradigm for multiple access in B5G and 6G networks [21]–[23]. RSMA has been realized in different forms for different multi-antenna settings [23]. The simplest form

of RSMA is based on 1-layer rate-splitting (RS)¹ which only requires one layer of successive interference cancellation (SIC) at each UE [24]. At the BS, RS splits the messages of UEs into two parts, a common part and a private part. The common parts of the UEs are combined together and encoded into common streams. The common streams are meant to be decoded by all UEs but not necessarily intended to all of them. The private parts are encoded independently into private streams and are meant to be decoded by the intended UE only (and treated as noise at the non-intended UEs). By adjusting the message split and power allocated to the common and private streams, RSMA allows to partially decode the interference and partially treat the interference as noise. From an information theoretic perspective, RSMA has been studied in-depth [24]–[29] and was shown to achieve the optimal degree of freedom (DoF) in multiple-input multiple-output (MISO) and MIMO broadcast channels (BC) with imperfect CSI [27], [28]. Motivated by the DoF optimality, communication theoretic performance of RSMA was investigated in [20], [25], [28], [30]–[32], and was shown to outperform the conventional multi-user MIMO strategy with linear precoders (also known as linearly precoded space division multiple access–SDMA) and power-domain non-orthogonal multiple access (PD-NOMA) in terms of SE and EE with imperfect CSI at the transmitter (CSIT) [20], [25], [30]. Interestingly, RSMA has been investigated to deal with the deleterious effects of multi-user interference in FDD MaMIMO [33], TDD cell-free MaMIMO [13] and to mitigate residual transceiver hardware impairments in TDD MaMIMO [34]. To the best of our knowledge, employing RSMA to address the issue of pilot contamination in TDD massive MIMO has not been investigated yet.

In this paper, motivated by the access behaviour of UEs in 5G, in turn the need to address the challenge of pilot contamination and the merits of RSMA in imperfect CSI, we propose a general² DL transmission framework of RSMA in a single cell TDD MaMIMO and investigate its performance as a PHY-layer strategy. Our main objective is to answer a simple question: *Can RSMA help in mitigating the deleterious effects of pilot contamination in TDD MaMIMO?*

A. Contributions

To investigate the efficacy of RSMA in TDD MaMIMO, we first analyze the DL performance of RSMA in TDD MaMIMO with perfect CSI, i.e., all UEs using orthogonal pilot sequences. To assess the performance in the presence of imperfect CSI, we assume that all UEs use the same pilot sequence for UL training.³ The aim is to consider the best case (orthogonal pilots) and the worst case (same pilot) scenario

¹Henceforth, 1-layer RS will be referred to as ‘RS’ for brevity.

²The framework is general in the sense that it is valid for any channel estimation and precoder design technique. The use of generalized RS from [20] instead of 1-layer RS is left for future work.

³The use of single pilot for UL transmission is not unprecedented in the literature of MaMIMO networks. [35] considers the case where all UEs utilize a single pilot and investigates the UL performance of a conventional strategy in a distributed MaMIMO network.

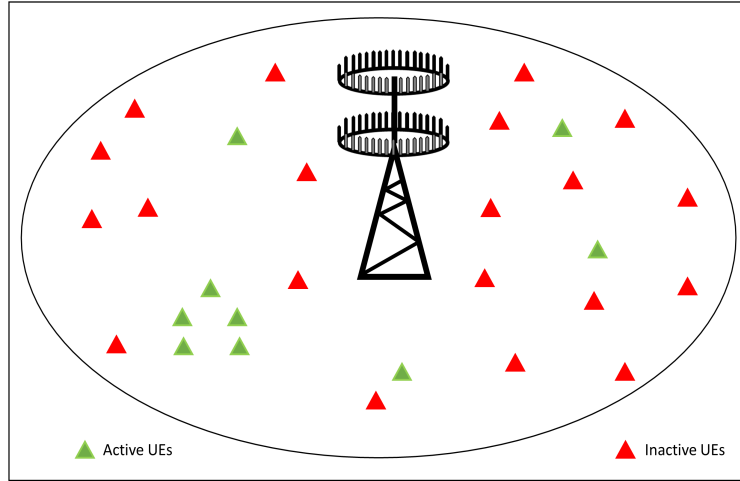


Figure 1: Illustration of massive access in a single-cell MaMIMO network for 5G and beyond.

in random access to determine the performance of RSMA and compare it with that of a conventional linearly precoded strategy. In this paper, we consider a single cell MaMIMO network and therefore assume no inter-cell pilot contamination. The main contributions of this paper are summarized as follows:

- We propose a novel system model employing RS in a TDD single-cell MaMIMO network. Based on the proposed system model, we derive the achievable SE expressions of RS and then obtain the capacity lower bound based on channel hardening (also known as hardening bound in [8]) for both the common and private streams. The derived hardening bounds are generalized for any UL channel estimation scheme and DL precoder design.
- To achieve a good SE performance with RS while keeping the computational complexity of precoder design low, we design the precoder for the common stream (common precoder) by maximizing the SE of the common stream and precoders for the private streams by employing maximum ratio (MR) transmission. The design of the common precoder solely depends on the channel statistics and therefore can be used for many coherence intervals.
- We propose three power allocation algorithms maximizing different network utilities for RS, namely, maximizing the sum-SE (MaxSum-SE), maximizing the product of signal to interference plus noise ratios (SINRs) (MaxSINR), and maximizing the minimum SE (MaxMin). For the MaxSum-SE problem, we propose a low-complexity heuristic algorithm to obtain the power allocation to maximize the sum of SE of all UEs. For the MaxSINR problem, to maximize the product of SINRs of the common and private streams, we equivalently transform it into a geometric programming (GP) problem and solve it optimally. Finally, the MaxMin problem is formulated to maximize the worst-case SE among UEs. The Max-Min problem is non-convex and is solved using the proposed successive convex approximation (SCA)-based algorithm.

- We compare the SE performance of the RS and NoRS⁴ strategies for different pilot sharing scenarios, spatial correlation settings and network topologies via extensive simulations. Numerical results illustrate the superiority of RS over NoRS in mitigating the deleterious effects of pilot contamination on DL transmission. This is the first work that proposes a general DL transmission framework of RSMA in TDD MaMIMO and investigates its efficacy as a pilot contamination mitigation strategy.

B. Organisation

The rest of the paper is organized as follows. In Section II, the system model is introduced. In Section III, SE expressions for the common and private streams are derived, and precoder design is proposed. Section IV discusses the power allocation problems formulated for the three aforementioned network utility functions and describes their respective optimization methodologies in detail. Numerical results are illustrated and discussed in Section V, while Section VI concludes the paper.

C. Notations

Matrices are denoted by boldface uppercase letters, column vectors are denoted by boldface lowercase letters and scalars are denoted by standard letters. Trace and determinant of matrix \mathbf{A} are denoted by $tr(\mathbf{A})$ and $\det(\mathbf{A})$, respectively. $diag(\mathbf{A})$ denotes the diagonal entries of the matrix. \mathbf{A}^T and \mathbf{A}^H denote the Transpose and Hermitian operators on the matrix \mathbf{A} , respectively. Euclidean norm of a vector \mathbf{a} is denoted as $\|\mathbf{a}\|$. \otimes denotes the Kronecker product and $vec(\mathbf{A})$ denotes vectorization of matrix \mathbf{A} . $\mathbb{E}_X\{Y\}$ is expectation of Y with respect to random variable X . $\mathbb{C}^{M \times N}$ and $\mathbb{R}^{M \times N}$ denote the sets of all $M \times N$ dimensional matrices with complex-valued and real-valued entries, respectively. The circularly symmetric complex gaussian (CSCG) distribution with mean μ and variance σ^2 is denoted as $\mathcal{CN}(\mu, \sigma^2)$.

II. SYSTEM MODEL

We consider a single-cell MaMIMO network operating in the TDD mode with a BS equipped with M transmit antennas simultaneously serving K single-antenna UEs in the same time-frequency resource block such that $M \gg K$. The UEs are indexed by the set $\mathcal{K} = \{1, \dots, K\}$. We use the standard block fading model and in each block, the channel between UE k and the BS, $\mathbf{g}_k \in \mathbb{C}^M$, is independently drawn from a block fading distribution as [8]

$$\mathbf{g}_k = \sqrt{\beta_k} \mathbf{h}_k \sim \mathcal{CN}(\mathbf{0}, \mathbf{R}_k), \quad (1)$$

⁴Henceforth, a conventional MaMIMO transmission strategy implemented using multi-user linear precoding [34] will be referred to as ‘NoRS’.

where $\mathbf{R}_k \in \mathbb{C}^{M \times M}$ denotes the spatial correlation matrix. Gaussian distribution is used to model the small-scale fading variations \mathbf{h}_k , while \mathbf{R}_k describes the large scale fading property which accounts for the path loss and shadowing effects. The normalized trace $\beta_k = \frac{1}{M} \text{tr}(\mathbf{R}_k)$ denotes the average channel gain between the BS and UE k . Since UEs operate under the standard cellular MaMIMO TDD protocol, each coherence block consists of τ channel uses, whereof τ_p are used for UL pilot transmission, τ_u for UL data transmission and τ_d for DL data transmission such that $\tau = \tau_p + \tau_u + \tau_d$ [8, Sec 2.1]. In this paper, we only consider UL pilot and DL data transmission and thus we set $\tau_u = 0$.

We assume that all UEs use a deterministic pilot sequence of length τ_p . The pilot sequence of UE k is denoted as $\{\phi_k \in \mathbb{C}^{\tau_p} \mid \forall k \in \mathcal{K}\}$. We assume that each element in the pilot sequence has a magnitude $1/\sqrt{\tau_p}$ to obtain constant power levels and therefore $\|\phi_k\|^2 = 1, \forall k \in \mathcal{K}$. We denote ρ_{ul} as the average UL transmit power available at each UE. The MMSE estimate of UE k at the BS when a single pilot sequence is employed by all UEs is computed as [8, Sec 3.2]

$$\hat{\mathbf{g}}_k = \mathbf{R}_k \mathbf{Q}^{-1} \left(\sum_{i=1}^K \mathbf{g}_i + \frac{1}{\sqrt{\rho_{\text{ul}}}} \mathbf{n}_{t,k} \right) \sim \mathcal{CN}(\mathbf{0}, \Phi_k), \quad (2)$$

where $\mathbf{n}_{t,k} \sim \mathcal{CN}(\mathbf{0}, \sigma_{\text{ul}}^2 \mathbf{I}_M)$, $\Phi_k = \mathbf{R}_k \mathbf{Q}^{-1} \mathbf{R}_k$, and $\mathbf{Q} = \sum_{i \in \mathcal{K}} \mathbf{R}_i + \frac{\sigma_{\text{ul}}^2}{\rho_{\text{ul}}} \mathbf{I}_M$. The channel estimate $\hat{\mathbf{g}}_k$ and the channel estimation error $\tilde{\mathbf{g}}_k = \mathbf{g}_k - \hat{\mathbf{g}}_k$ are independent random variables with distributions $\mathcal{CN}(\mathbf{0}, \Phi_k)$ and $\mathcal{CN}(\mathbf{0}, \mathbf{R}_k - \Phi_k)$, respectively. Since all UEs use the same pilot sequence, they contaminate each others' channel estimates, which makes their channel estimates statistically dependent. Assuming \mathbf{R}_i to be invertible, it follows that the channel estimate of UE k at the BS can be written as,

$$\hat{\mathbf{g}}_k = \mathbf{R}_k \mathbf{R}_i^{-1} \hat{\mathbf{g}}_i \quad i \in \mathcal{K}, \quad (3)$$

and therefore, $\mathbb{E}\{\hat{\mathbf{g}}_i \hat{\mathbf{g}}_k^H\} = \mathbf{R}_i \mathbf{Q}^{-1} \mathbf{R}_k$ [1], [8].

Similarly, if UEs are assigned orthogonal pilots for UL training, the channel estimate of UE k is computed as

$$\hat{\mathbf{g}}_k = \mathbf{R}_k \mathbf{Q}_k^{-1} \left(\mathbf{g}_k + \frac{1}{\sqrt{\rho_{\text{ul}}}} \mathbf{n}_{t,k} \right) \sim \mathcal{CN}(\mathbf{0}, \Phi_k), \quad (4)$$

where $\Phi_k = \mathbf{R}_k \mathbf{Q}_k^{-1} \mathbf{R}_k$ and $\mathbf{Q}_k^{-1} = \mathbf{R}_k + \frac{\sigma_{\text{ul}}^2}{\rho_{\text{ul}}} \mathbf{I}_M$. Since the pilots are orthogonal to each other, channel estimate of one UE is not contaminated by the channel of other UE and thus, the estimates are not statistically dependent.

III. RATE-SPLITTING IN DL TRANSMISSION

For DL transmission, we use the RS strategy described in [20], [24] where the message of UE k , $\forall k \in \mathcal{K}$ denoted by W_k is split into two parts, a common part $W_{c,k}$ and a private part $W_{p,k}$. The common parts of all UEs, $\{W_{c,1}, \dots, W_{c,K}\}$, are combined together to form a single common message denoted

as W_c and then encoded into a single common stream $s_c \in \mathbb{C}$ using a common codebook such that $\mathbb{E}\{|s_c|^2\} = 1$. The common stream is meant to be decoded by all UEs (but not necessarily intended to all of them). The private part of UE k is encoded independently into the private stream $s_k \in \mathbb{C}$ such that $\mathbb{E}\{|s_k|^2\} = 1, \forall k \in \mathcal{K}$ and is meant to be decoded by the corresponding UE only. The DL transmission framework of the RS strategy with K UEs is illustrated in Fig. 2. The resulting transmitted signal is written as:

$$\mathbf{x} = \sqrt{\rho_c} \mathbf{w}_c s_c + \sum_{k=1}^K \sqrt{\rho_k} \mathbf{w}_k s_k, \quad (5)$$

where $\mathbf{w}_c \in \mathbb{C}^M$ is the precoder of the common stream such that $\mathbb{E}\{\|\mathbf{w}_c\|^2\} = 1$. $\mathbf{w}_k \in \mathbb{C}^M$ is the precoder for the private stream of UE k such that $\mathbb{E}\{\|\mathbf{w}_k\|^2\} = 1, \forall k \in \mathcal{K}$ and it determines the spatial directivity of UE k . Note that the precoder normalization for both common and private precoders is taken as such for analytical tractability [8, Sec 4.3]. The powers allocated to the common and private streams are denoted by ρ_c and $\rho_k, \forall k \in \mathcal{K}$, respectively. We define the DL transmit power constraint as

$$\rho_c + \sum_{k=1}^K \rho_k \leq \rho_{\text{DL}}, \quad (6)$$

where ρ_{DL} is the total transmit power available at the BS in DL. At the UE side, the received signal $y_k \in \mathbb{C}$ at UE k is given by

$$y_k = \sqrt{\rho_c} \mathbf{g}_k^H \mathbf{w}_c s_c + \sum_{i=1}^K \sqrt{\rho_i} \mathbf{g}_k^H \mathbf{w}_i s_i + n_k, \quad (7)$$

where $n_k \in \mathcal{CN}(0, \sigma_{n,k}^2)$ is the noise at UE k . Without loss of generality, we assume noise variances across UEs to be $\sigma_{n,k}^2 = \sigma_n^2, \forall k \in \mathcal{K}$. At UE k , first the common stream is decoded into \widehat{W}_c by treating the interference from all private streams as noise. After decoding and successfully removing the common stream using SIC, UE k decodes its own private stream into $\widehat{W}_{p,k}$ by treating the private streams of other UEs as noise. UE k reconstructs its message by extracting $\widehat{W}_{c,k}$ from \widehat{W}_c , and combining it with $\widehat{W}_{p,k}$ to form \widehat{W}_k .

A. Spectral Efficiency

Assuming channel reciprocity within a coherence block, the BS then uses the estimates of UL channels to compute the precoders for DL data transmission. Since the UE is unaware⁵ of its exact channel, we

⁵In TDD MaMIMO, due to asymptotic channel hardening, instantaneous CSI is not needed at the receiver and knowledge of statistical properties can be used to find good estimate of the channel [36] (and references there in). This assumption significantly reduces the resource (power and training duration) overhead and therefore is a widely used assumption in the literature of MaMIMO [8], [36].

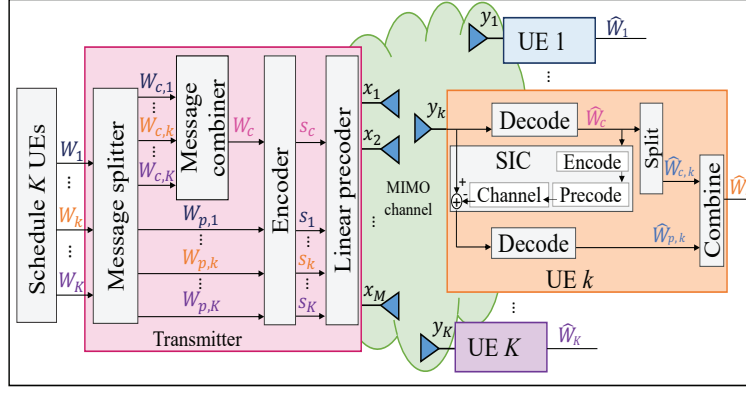


Figure 2: K-UE DL transmission framework of RS [20].

assume that UE k has knowledge of the ergodic effective precoded channels $\mathbb{E}\{\mathbf{g}_k^H \mathbf{w}_c\}$ and $\mathbb{E}\{\mathbf{g}_k^H \mathbf{w}_k\}$ [8]. Under this assumption, the received signal at UE k can then be expressed as

$$y_{c,k} = \sqrt{\rho_c} \mathbb{E}\{\mathbf{g}_k^H \mathbf{w}_c\} s_c + \sqrt{\rho_c} (\mathbf{g}_k^H \mathbf{w}_c - \mathbb{E}\{\mathbf{g}_k^H \mathbf{w}_c\}) s_c + \sum_{i=1}^K \sqrt{\rho_i} \mathbf{g}_k^H \mathbf{w}_i s_i + n_k, \quad (8)$$

and after SIC⁶ of the common stream, the received signal at UE k becomes

$$y_{p,k} = \sqrt{\rho_k} \mathbb{E}\{\mathbf{g}_k^H \mathbf{w}_k\} s_k + \sqrt{\rho_k} (\mathbf{g}_k^H \mathbf{w}_k - \mathbb{E}\{\mathbf{g}_k^H \mathbf{w}_k\}) s_k + \sqrt{\rho_c} (\mathbf{g}_k^H \mathbf{w}_c - \mathbb{E}\{\mathbf{g}_k^H \mathbf{w}_c\}) s_c + \sum_{i \neq k}^K \sqrt{\rho_i} \mathbf{g}_k^H \mathbf{w}_i s_i + n_k. \quad (9)$$

The limited knowledge of the channel at UE makes it hard to characterize the DL SE for both common and private streams. Therefore, we compute a lower bound to the capacity, known as the hardening bound

$$\text{SE}_{c,k} = \frac{\tau_d}{\tau} \log(1 + \gamma_{c,k}), \quad (10)$$

$$\text{SE}_{p,k} = \frac{\tau_d}{\tau} \log(1 + \gamma_{p,k}), \quad (11)$$

where $\gamma_{c,k}$ and $\gamma_{p,k}$ are the effective DL SINR lower bounds⁷ of the common and private streams at UE k , respectively. With the expectations computed over channel realizations, $\gamma_{c,k}$ and $\gamma_{p,k}$ are given by (13) and (14), respectively. The expectations of the effective precoded channels are with respect to the channel realizations and can be calculated using Monte Carlo simulations. As the common stream is decoded by all UEs, the achievable SE for the common stream (common SE) is defined as

$$\text{SE}_c = \frac{\tau_d}{\tau} \log(1 + \gamma_c), \quad (12)$$

⁶Since the UE does not have perfect knowledge of the CSI, SIC of the common stream is not perfect. As a result, residual interference from the common stream still remains after SIC and is reflected in equation (9).

⁷Using Corollary 1.3, Theorem 4.6 (and its proof in Appendix C.3.6) of [8] derives the lower bound of the DL ergodic channel capacity of a UE for the NoRS transmission strategy. The proof can be directly extended for RS by utilizing the effective SINR expressions (13) and (14) of common and private streams derived here and equation (1.9) of [8].

$$\gamma_{c,k} = \frac{\rho_c |\mathbb{E}\{\mathbf{g}_k^H \mathbf{w}_c\}|^2}{\sum_{i=1}^K \rho_i \mathbb{E}\{|\mathbf{g}_k^H \mathbf{w}_i|^2\} + \rho_c (\mathbb{E}\{|\mathbf{g}_k^H \mathbf{w}_c|^2\} - |\mathbb{E}\{\mathbf{g}_k^H \mathbf{w}_c\}|^2) + \sigma_n^2}, \quad (13)$$

$$\gamma_{p,k} = \frac{\rho_k |\mathbb{E}\{\mathbf{g}_k^H \mathbf{w}_k\}|^2}{\sum_{i=1}^K \rho_i \mathbb{E}\{|\mathbf{g}_k^H \mathbf{w}_i|^2\} - \rho_k |\mathbb{E}\{\mathbf{g}_k^H \mathbf{w}_k\}|^2 + \rho_c (\mathbb{E}\{|\mathbf{g}_k^H \mathbf{w}_c|^2\} - |\mathbb{E}\{\mathbf{g}_k^H \mathbf{w}_c\}|^2) + \sigma_n^2}, \quad (14)$$

where $\gamma_c = \min_{k \in \mathcal{K}} \gamma_{c,k}$. Note that the hardening bounds hold for any choice of channel estimator and precoder design.

B. Precoder Design

The SE expressions in (11) and (12) are general and can be utilized for any choice of common and private precoders. Due to the massive number of transmit antennas at the BS, high dimensional optimization of common and private precoders is infeasible in MaMIMO. Instead, low-complexity precoder design is desired for both common and private streams. Therefore, for private streams, we choose MR transmission precoders as they have low-complexity, achieve good SE performance with a high number of transmit antennas, and allow closed-form computation of the expectations in the SINR expressions [1], [8]. The MR precoder for the private stream of UE k is defined as

$$\mathbf{w}_k = \frac{\hat{\mathbf{g}}_k}{\sqrt{\mathbb{E}\{\|\hat{\mathbf{g}}_k\|^2\}}} = \frac{\hat{\mathbf{g}}_k}{\sqrt{\text{tr}(\mathbf{\Phi}_k)}}. \quad (15)$$

With MR precoders, the closed-form expectations $\mathbb{E}\{|\mathbf{g}_k^H \mathbf{w}_k|^2\}$ and $|\mathbb{E}\{\mathbf{g}_k^H \mathbf{w}_i\}|^2$, $\forall i, k \in \mathcal{K}$ are given by

$$|\mathbb{E}\{\mathbf{g}_k^H \mathbf{w}_k\}|^2 = \text{tr}(\mathbf{\Phi}_k), \quad (16)$$

$$\mathbb{E}\{|\mathbf{g}_k^H \mathbf{w}_i|^2\} = \frac{\text{tr}(\mathbf{R}_k \mathbf{\Phi}_i) + |\text{tr}(\mathbf{R}_k \mathbf{Q}^{-1} \mathbf{R}_i)|^2}{\text{tr}(\mathbf{\Phi}_i)}. \quad (17)$$

Note that only large scale fading coefficients are needed to calculate the closed-form expectations and in turn the hardening bounds.

Next we look at the design of the common precoder. Since the common stream is to be decoded by all UEs, considering equation (12), an ideal precoder for the common stream would be the one that maximizes the common SE. Consequently, the common precoder design problem can be formulated as

$$\max_{\mathbf{w}_c} \min_k \gamma_{c,k}, \quad (18a)$$

$$s.t. \quad \mathbb{E}\{\|\mathbf{w}_c\|^2\} = 1. \quad (18b)$$

Unfortunately, obtaining the optimal solution to problem (18) is computationally demanding because of the beamforming gain uncertainty term in the denominator of the SINR expressions of the common

stream, $\rho_c(\mathbb{E}\{|\mathbf{g}_k^H \mathbf{w}_c|^2\} - |\mathbb{E}\{\mathbf{g}_k^H \mathbf{w}_c\}|^2)$, which makes problem (18) intractable to solve. Moreover, such optimization will undesirably increase the time required for computing the common precoder. For ease of computation, a sub-optimal solution to problem (18) can be obtained by assuming that the difference $(\mathbb{E}\{|\mathbf{g}_k^H \mathbf{w}_c|^2\} - |\mathbb{E}\{\mathbf{g}_k^H \mathbf{w}_c\}|^2)$ is very small and can be neglected to make the problem tractable.⁸ Following this assumption, problem (18) can be formulated as

$$\begin{aligned} \max_{\mathbf{w}_c} \min_k \quad & \pi_k |\mathbb{E}\{\mathbf{g}_k^H \mathbf{w}_c\}|^2 \\ \text{s.t.} \quad & \mathbb{E}\{\|\mathbf{w}_c\|^2\} = 1, \end{aligned} \quad (19)$$

where

$$\pi_k = \frac{1}{\sum_{i=1}^K \mathbb{E}\{|\mathbf{g}_k^H \mathbf{w}_i|^2\} + \sigma_n^2}. \quad (20)$$

We consider a weighted MR approach and design the common precoder in the span of subspace of the estimated channel vectors $\{\hat{\mathbf{g}}_i \mid \forall i \in \mathcal{K}\}$ at the BS as

$$\mathbf{w}_c = \Omega \sum_{i=1}^K a_i \hat{\mathbf{g}}_i, \quad (21)$$

where Ω is the scaling factor required to satisfy the constraint $\mathbb{E}\{\|\mathbf{w}_c\|^2\} = 1$.⁹ By substituting (21) into $\mathbb{E}\{\mathbf{g}_k^H \mathbf{w}_c\}$, we rewrite (19) as

$$\max_{\{a_i \mid \forall i \in \mathcal{K}\}} \min_k \quad \Omega^2 \pi_k \left| \sum_{i=1}^K a_i \mathbf{U}(i, k) \right|^2, \quad (22a)$$

$$\text{s.t.} \quad \mathbb{E}\{\|\mathbf{w}_c\|^2\} = 1, \quad (22b)$$

where

$$\mathbf{U}(i, k) = \mathbb{E}\{\hat{\mathbf{g}}_k^H \hat{\mathbf{g}}_i\}, \forall i, k \in \mathcal{K}. \quad (23)$$

For simplicity, we ignore Ω^2 in (22). By introducing an auxiliary variable t , we obtain the convex form of the objective and constraints of problem (22) and equivalently transform it into the following convex optimization problem:

$$\max_{\mathbf{a}, t > 0} \quad t, \quad (24a)$$

$$\text{s.t.} \quad \mathbf{a}^T \mathbf{U}(:, k) \geq t, \quad \forall k \in \mathcal{K}, \quad (24b)$$

⁸The assumption of neglecting beamforming gain uncertainty $(\mathbb{E}\{|\mathbf{g}_k^H \mathbf{w}_c|^2\} - |\mathbb{E}\{\mathbf{g}_k^H \mathbf{w}_c\}|^2)$ of the common stream at UE k is restricted to the common precoder design at the BS and is only considered to make problem (18) tractable. The assumption is not a part of the system model or SE calculations at the BS or at the UEs.

⁹Reference [33] also adopts the weighted MR approach for common precoder design of RSMA in FDD MaMIMO. In [33], the closed-form computation of the coefficients $a_i, \forall i \in \mathcal{K}$ is done based on the instantaneous SINR expressions. Moreover, DL training allows the UE to have the knowledge of the effective precoded channel. In contrast, we consider no DL training at the UE, and calculate common precoder coefficients utilizing the hardening bounds of the common and private SINRs.

where $\mathbf{a} = [a_1, \dots, a_K]^T$. We solve problem (24) to obtain \mathbf{a}^* which is then used to compute the optimal common precoder \mathbf{w}_c^* . For the scenario of every UE using the same pilot for UL channel estimation, we have $\mathbf{U}(i, k) = \text{tr}(\mathbf{R}_i \mathbf{Q}^{-1} \mathbf{R}_k)$ and the common precoder is computed as

$$\mathbf{w}_c^* = \frac{\sum_{i=1}^K a_i^* \hat{\mathbf{g}}_i}{\sqrt{\sum_{i=1}^K \sum_{j=1}^K a_i^* a_j^* \text{tr}(\mathbf{R}_i \mathbf{Q}^{-1} \mathbf{R}_j)}}. \quad (25)$$

Using (25), we compute the closed-form expressions of the expectations $\mathbb{E}\{\mathbf{g}_k^H \mathbf{w}_c^*\}$ and $\mathbb{E}\{|\mathbf{g}_k^H \mathbf{w}_c^*|^2\}$ which are solely dependent on the channel statistics. Appendix A specifies the derivation of these expectations.

With orthogonal pilots, we have $\{\mathbf{U}(i, k) = \text{tr}(\Phi_i) \mid i = k\}$ and $\{\mathbf{U}(i, k) = 0 \mid \forall k \neq i\}$. To avoid redundancy, we do not elaborate on the common precoder calculation for orthogonal pilots. Similarly, the common precoder design problem in (19) can be solved for any pilot sharing scenario by calculating the corresponding value of \mathbf{U} using (23). The computation of common precoder coefficients, \mathbf{a} , solely depends on the large scale fading coefficients. Therefore, \mathbf{a} only needs to be calculated once. Consequently, the common precoder can be calculated using \mathbf{a} and (21) for many coherence intervals, until the channel statistics change. Such precoder design keeps the overall time and computational burden very low.

IV. POWER ALLOCATION

In this section, we aim at obtaining the power allocation coefficients $\boldsymbol{\rho} = \{\rho_c, \rho_1, \dots, \rho_K\}$ for the common and private streams of RS by considering different utility functions as the optimization objectives. Following [8], we consider utility functions and consequently formulate power allocation schemes for RS that aim to maximize the sum-SE or maximize user fairness or strike a balance between maximizing sum-SE performance and fairness. We define a network utility function as $U(\text{SE}_1, \dots, \text{SE}_K)$ which takes common and private SEs as input and returns a scalar that measures the utility as the output [8]. The utility functions are defined as:

$$U(\text{SE}_1, \dots, \text{SE}_K) : \begin{cases} \text{SE}_c + \sum_{k=1}^K \text{SE}_k, & \text{Sum-SE} \\ \left(\prod_{k=1}^K \gamma_{p,k} \right) \gamma_c, & \text{Product of SINRs} \\ \min_{k \in \mathcal{K}} \text{SE}_k + C_k, & \text{Minimum SE,} \end{cases} \quad (26)$$

where γ_c and $\gamma_{p,k}, \forall k \in \mathcal{K}$ are effective SINRs of the common and private streams, respectively. C_k is the share of the common SE allocated to UE k , $k \in \mathcal{K}$ such that $\sum_{k \in \mathcal{K}} C_k = \text{SE}_c$. We respectively formulate and solve the power allocation problems for RS with the aim of maximizing the three different utility functions in (26), i.e., 1) Maximizing sum-SE (MaxSum-SE), 2) Maximizing product of SINRs (MaxSINR) and 3) Maximizing the minimum SE (MaxMin). All power allocation schemes designed in this paper will

hold for any channel estimation and precoder design method. Moreover, each power allocation scheme is solely dependent on the channel statistics and therefore can be used for many coherence intervals. We define the utility maximization problem as

$$\begin{aligned} \max_{\boldsymbol{\rho}} \quad & U(\mathbf{SE}_1, \dots, \mathbf{SE}_K), \\ \text{s.t.} \quad & \rho_c + \sum_{i=1}^K \rho_i \leq \rho_{\text{dL}}. \end{aligned} \quad (27)$$

For simplicity, we first rewrite equations (13) and (14) as

$$\gamma_{c,k} = \frac{\rho_c a_{c,k}}{\sum_{i=1}^K \rho_i b_{ki}^c + \rho_c I_{c,k} + \sigma_n^2}, \quad (28)$$

$$\gamma_{p,k} = \frac{\rho_k a_{p,k}}{\sum_{i=1}^K \rho_i b_{ki}^p + \rho_c I_{c,k} + \sigma_n^2}, \quad (29)$$

respectively, where

$$\begin{aligned} a_{c,k} &= |\mathbb{E}\{\mathbf{g}_k^H \mathbf{w}_c\}|^2, \quad \forall k \in \mathcal{K}, \\ a_{p,k} &= |\mathbb{E}\{\mathbf{g}_k^H \mathbf{w}_k\}|^2, \quad \forall k \in \mathcal{K}, \end{aligned} \quad (30)$$

$$\begin{aligned} b_{ki}^c &= \mathbb{E}\{|\mathbf{g}_k^H \mathbf{w}_i|^2\}, \quad \forall k \in \mathcal{K}, \\ b_{ki}^p &= \begin{cases} \mathbb{E}\{|\mathbf{g}_k^H \mathbf{w}_i|^2\}, & i \neq k, \forall i, k \in \mathcal{K}, \\ \mathbb{E}\{|\mathbf{g}_k^H \mathbf{w}_k|^2\} - |\mathbb{E}\{\mathbf{g}_k^H \mathbf{w}_k\}|^2, & i = k, \forall i, k \in \mathcal{K}, \end{cases} \end{aligned} \quad (31)$$

and

$$I_{c,k} = \mathbb{E}\{|\mathbf{g}_k^H \mathbf{w}_c|^2\} - |\mathbb{E}\{\mathbf{g}_k^H \mathbf{w}_c\}|^2, \quad \forall k \in \mathcal{K}. \quad (32)$$

Note that, while the channel estimates and the closed-form expressions of the expectations depend on whether UEs are using the same pilot or orthogonal pilots, the power allocation algorithms are not affected by the choice of pilot sequences or precoder design¹⁰. As aforementioned, only large scale fading characteristics are used to design the power allocation algorithms of RS in MaMIMO. Therefore, the advantage of being able to design complex yet feasible power allocation schemes which can be used for multiple coherence blocks is retained for RS as well with our proposed transmission framework. In the following, we formulate the three power allocation problems for RS and specify the algorithms proposed to solve the corresponding problems.

¹⁰While the power allocation algorithms themselves are unaffected by the choice of pilots or precoders, the power allocation between the common and private precoders will be influenced by both.

A. Maximizing sum-SE

For any given channel estimation technique, precoding scheme and values of $a_{c,k}$, $a_{p,k}$, b_{ki}^c , b_{ki}^p and $I_{c,k}$, the sum-SE can be written as

$$\text{SE} = \text{SE}_c + \sum_{k=1}^K \text{SE}_{p,k}, \quad (33)$$

where SE_c and $\text{SE}_{p,k}$ are defined in (12) and (11), respectively. The MaxSum-SE problem can therefore be formulated as

$$\max_{\boldsymbol{\rho}} \text{SE}_c(\boldsymbol{\rho}) + \sum_{k=1}^K \text{SE}_{p,k}(\boldsymbol{\rho}), \quad (34a)$$

$$s.t. \quad \rho_c + \sum_{i=1}^K \rho_i \leq \rho_{\text{dL}}. \quad (34b)$$

We here consider a heuristic low-complexity power allocation strategy where power allocated to the common stream is $\rho_c = (1-\zeta)\rho_{\text{dL}}$ and the power allocated to each private stream is $\rho_k = \zeta\rho_{\text{dL}}/K$, $\forall k \in \mathcal{K}$, where $\zeta \in [0, 1]$ is a scalar. An exhaustive search for ζ is then considered to obtain the power allocation between the common and private streams for which the sum-SE is maximum. Such an approach does not require optimization techniques and maintains a low complexity, which is desirable to many possible use cases of future wireless networks. Algorithm 1 outlines the MaxSum-SE power allocation algorithm of RS that gives the power allocation between the common stream and private streams, and ultimately obtains the sum-SE. To be thorough, the power allocation coefficients in (34) are also obtained using an optimization technique detailed in Appendix B and a comparison with Algorithm 1 is provided in terms of sum-SE and time consumed to obtain the sum-SE.

Algorithm 1 MaxSum-SE

- 1: **Initialize** $n \leftarrow 0$, $\zeta \leftarrow 0$, $\Delta \leftarrow 0.05$, $\text{SE}^{[n]}$
 - 2: **Iterate**
 - 3: $n \leftarrow n + 1$;
Obtain $\rho_c \leftarrow (1 - \zeta)\rho_{\text{dL}}$ and $\rho_k \leftarrow \frac{\zeta\rho_{\text{dL}}}{K}$, $\forall k \in \mathcal{K}$;
Calculate $\text{SE}^{[n]}$ using (28), (29) and (33);
 - 4: **Update** $\text{SE}^{[n]} \leftarrow \max(\text{SE}^{[n]}, \text{SE}^{[n-1]})$, $\zeta \leftarrow \zeta + \Delta$
 - 5: **Until** $\zeta = 1$
-

B. Maximizing product of SINRs

We next consider MaxSINR¹¹ power allocation which aims to strike a balance between maximizing the sum-SE and maintaining fairness in the network. For any given channel estimation, precoding scheme and values of $a_{c,k}$, $a_{p,k}$, b_{ki}^c , b_{ki}^p and $I_{c,k}$, MaxSINR utility function maximization problem of RS can be written as

$$\max_{\gamma_c, \boldsymbol{\rho}} \left(\prod_{i=1}^K \gamma_{p,i} \right) \gamma_c \quad (35a)$$

$$s.t. \quad \gamma_c \leq \gamma_{c,k}, \forall k \in \mathcal{K}, \quad (35b)$$

$$\rho_c + \sum_{i=1}^K \rho_i \leq \rho_{dL}, \quad (35c)$$

where $\gamma_{c,k}$ and $\gamma_{p,k}$ are defined in (28) and (29), respectively. Constraint (35b) ensures that the common stream is decodable at all UEs. Since problem (35) is non-convex, we transform it into an equivalent GP form by introducing auxiliary variables o_c and $\mathbf{o}_p = [o_{p,1}, \dots, o_{p,K}]$ to respectively represent the common SINR and the private SINR vector such that

$$o_{p,k} \left(\sum_{i=1}^K \rho_i b_{ki}^p + \rho_c I_{c,k} + \sigma_n^2 \right) \leq \rho_k a_{p,k}, \forall k \in \mathcal{K}, \quad (36a)$$

$$o_c \left(\sum_{i=1}^K \rho_i b_{ki}^c + \rho_c I_{c,k} + \sigma_n^2 \right) \leq \rho_c a_{c,k}, \forall k \in \mathcal{K}. \quad (36b)$$

Using (36a) and (36b), we transform problem (35) equivalently into a GP problem given by

$$\max_{\boldsymbol{\rho}, \mathbf{o}_p, o_c} \left(\prod_{i=1}^K o_{p,i} \right) o_c \quad (37a)$$

$$s.t. \quad o_{p,k} \frac{\left(\sum_{i=1}^K \rho_i b_{ki}^p + \rho_c I_{c,k} + \sigma_n^2 \right)}{\rho_k a_{p,k}} \leq 1, \forall k \in \mathcal{K}, \quad (37b)$$

$$o_c \frac{\left(\sum_{i=1}^K \rho_i b_{ki}^c + \rho_c I_{c,k} + \sigma_n^2 \right)}{\rho_c a_{c,k}} \leq 1, \forall k \in \mathcal{K}, \quad (37c)$$

$$\rho_c + \sum_{i=1}^K \rho_i \leq \rho_{dL}. \quad (37d)$$

The objective function and the constraints in problem (37) are posynomials and therefore it is a GP problem [37]. We use CVX, a tool used to solve disciplined convex programs in Matlab for finding the solution of the above GP problem and obtaining the optimal power allocation $\boldsymbol{\rho}^*$ that maximizes product of SINRs utility function for RS in MaMIMO. Algorithm 2 outlines the MaxSINR power allocation

¹¹Product of SINRs aims to maximize the sum-SE where “1+” term is neglected in every SE expression. While ignoring “1+” term has a minuscule affect on UEs with high SINRs, UEs with lower SINRs have their SEs underestimated [8]. As a result, MaxSINR power allocation would lead to higher SE for weaker UEs compared to MaxSum-SE.

algorithm of RS. It should be highlighted that in a GP, there is an implicit constraint that the optimization variables are positive, i.e., here $\rho_i > 0, \forall i \in \mathcal{K}$ and $\rho_c > 0$. This non zero power allocation to all the streams assures a non zero SE to each UE thereby ensuring fairness in the network.

Algorithm 2 MaxSINR: GP Algorithm

- 1: **Declare** ρ_c, \mathbf{o}_p
 Transform (35) into GP problem (37) using (36a) and (36b);
 - 2: **Solve** (37) using CVX to obtain $\boldsymbol{\rho}$
 - 3: **Calculate** SE_c and $\text{SE}_{p,k}$
-

C. Maximizing the minimum SE

MaxSINR optimization, as aforementioned, aims to strike a balance between maximizing the sum-SE and fairness among UEs. We next consider MaxMin optimization problem whose objective is to achieve the maximum user fairness. The maximization of minimum SE problem of RS for any given channel estimation, precoding scheme and values of $a_{c,k}, a_{p,k}, b_{ki}^c, b_{ki}^p$ and $I_{c,k}$ can be expressed as

$$\max_{\boldsymbol{\rho}, \mathbf{c}} \min_k \text{SE}_{p,k} + C_k, \quad (38a)$$

$$s.t. \quad C_1 + \dots + C_K \leq \text{SE}_{c,k}, \quad \forall k \in \mathcal{K}, \quad (38b)$$

$$\rho_c + \sum_{i=1}^K \rho_i \leq \rho_{\text{dL}}, \quad (38c)$$

$$\mathbf{c} \geq \mathbf{0}, \quad (38d)$$

where $\mathbf{c} = [C_1, \dots, C_K]$ is the common SE vector with C_k being the share of the common SE allocated to UE k such that $\text{SE}_c = \sum_{i=1}^K C_i$. Constraint (38b) ensures that the common stream is decoded at all UEs. Our aim is to jointly optimize the power allocated to the common stream ρ_c , private streams $\rho_i, \forall i \in \mathcal{K}$, and the common SE vector \mathbf{c} .

The MaxMin problem (38) described above is a non-convex problem due to the presence of logarithmic and fractional SE expressions $\text{SE}_{p,k}$ and $\text{SE}_{c,k}$. Motivated by the SCA algorithm adopted in [30], [38]¹², we propose a SCA-based power allocation algorithm to solve problem (38). To achieve the best possible performance, we introduce auxiliary variables to transform the MaxMin problem into its equivalent form and approximate the transformed problem into convex sub-problems, which are solved iteratively until convergence. Next we delineate the transformation, approximations, and procedure to solve the resultant problem.

¹²Both [30], [38] formulate the SCA algorithm for precoder design in multi-user MISO networks with perfect CSIT.

We introduce an auxiliary variable t , vectors $\boldsymbol{\alpha}_c = [\alpha_{c,1}, \dots, \alpha_{c,K}]$, and $\boldsymbol{\alpha}_p = [\alpha_{p,1}, \dots, \alpha_{p,K}]$ representing the minimum SE, SE of the common stream at UEs and private SEs of UEs, respectively. Similarly, we introduce $\mathbf{r}_c = [r_{c,1}, \dots, r_{c,K}]$ and $\mathbf{r}_p = [r_{p,1}, \dots, r_{p,K}]$, representing 1 plus SINR values for the common and private streams of UEs, respectively. Problem (38) is equivalently transformed as

$$\max_{\substack{\boldsymbol{\rho}, \mathbf{c}, \boldsymbol{\alpha}_p, \boldsymbol{\alpha}_c, \\ \mathbf{r}_p, \mathbf{r}_c, t}} t \quad (39a)$$

$$s.t. \alpha_{p,k} + C_k \geq t, \quad \forall k \in \mathcal{K}, \quad (39b)$$

$$\alpha_{c,k} \geq \sum_{k \in \mathcal{K}} C_k, \quad \forall k \in \mathcal{K}, \quad (39c)$$

$$r_{p,k} - 2^{\frac{\tau}{\tau_d} \alpha_{p,k}} \geq 0 \quad \forall k \in \mathcal{K}, \quad (39d)$$

$$r_{c,k} - 2^{\frac{\tau}{\tau_d} \alpha_{c,k}} \geq 0 \quad \forall k \in \mathcal{K}, \quad (39e)$$

$$\frac{\rho_c a_{c,k}}{\sum_{i=1}^K \rho_i b_{ki}^c + \rho_c I_{c,k} + \sigma_n^2} \geq r_{c,k} - 1, \quad \forall k \in \mathcal{K}, \quad (39f)$$

$$\frac{\rho_k a_{p,k}}{\sum_{i=1}^K \rho_i b_{ki}^p + \rho_c I_{c,k} + \sigma_n^2} \geq r_{p,k} - 1, \quad \forall k \in \mathcal{K}, \quad (39g)$$

$$\mathbf{c} \geq \mathbf{0}, \quad (39h)$$

$$\rho_c + \sum_{i=1}^K \rho_i \leq \rho_{dL}. \quad (39i)$$

Here, (39) aims to maximize the lower bound of the objective function (38a) under the constraints (38b)–(38d). The equivalence between (38) and (39) is established based on the fact that at optimum, equality holds for constraints (39b)–(39g) and (39i). Next, we deal with the non-convex constraints (39f) and (39g) by further introducing auxiliary variables $\boldsymbol{\chi}_c = \{\chi_{c,1}, \dots, \chi_{c,K}\}$ and $\boldsymbol{\chi}_p = \{\chi_{p,1}, \dots, \chi_{p,K}\}$ representing the noise plus interference experienced by the common stream at UE sides and private streams, respectively. In addition, we introduce variables $\boldsymbol{\nu} = \{\nu_c, \nu_1, \dots, \nu_K\}$ such that $\nu_c^2 = \rho_c$ and $\nu_k^2 = \rho_k, \forall k \in \mathcal{K}$. Consequently, constraints (39f) can be equivalently written as

$$\frac{\nu_c^2 a_{c,k}}{\chi_{c,k}} \geq r_{c,k} - 1, \quad \forall k \in \mathcal{K}, \quad (40a)$$

$$\chi_{c,k} \geq \sum_{i=1}^K \nu_i^2 b_{ki}^c + \nu_c^2 I_{c,k} + \sigma_n^2, \quad \forall k \in \mathcal{K}. \quad (40b)$$

Similarly, for the private streams, constraint (39g) can be equivalently written as

$$\frac{\nu_k^2 a_{p,k}}{\chi_{p,k}} \geq r_{p,k} - 1, \quad \forall k \in \mathcal{K}, \quad (41a)$$

$$\chi_{p,k} \geq \sum_{i=1}^K \nu_i^2 b_{ki}^p + \nu_c^2 I_{c,k} + \sigma_n^2, \quad \forall k \in \mathcal{K}. \quad (41b)$$

The transmit power constraint, i.e., (39i) can be written as

$$\nu_c^2 + \sum_{i=1}^K \nu_i^2 \leq \rho_{\text{dL}}. \quad (42)$$

Therefore, problem (38) is equivalently transformed into

$$\begin{aligned} & \max_{\substack{\boldsymbol{\nu}, \mathbf{c}, \boldsymbol{\alpha}_p, \boldsymbol{\alpha}_c, \\ \mathbf{r}_p, \mathbf{r}_c, \boldsymbol{\chi}_p, \boldsymbol{\chi}_c, t}} t \\ & \text{s.t. } (39b), (39c), (39d), (39e), (39h), \\ & \quad (40a), (40b), (41a), (41b), (42). \end{aligned} \quad (43)$$

The constraints of the transformed problem (43) are convex with the exception of (40a) and (41a). Hence, in each iteration, we use the first-order Taylor approximation to linearly approximate the non-convex parts of these constraints. Linear approximation of the left side of constraint (40a) is given by

$$\frac{\nu_c^2 a_{c,k}}{\chi_{c,k}} \geq a_{c,k} \left(\frac{2\nu_c^{[n]}}{\chi_{c,k}^{[n]}} \nu_c - \frac{(\nu_c^{[n]})^2}{(\chi_{c,k}^{[n]})^2} \chi_{c,k} \right) \triangleq \Psi_{c,k}^{[n]}(\nu_c, \chi_{c,k}), \quad (44)$$

where $(\nu_c^{[n]}, \chi_{c,k}^{[n]})$ are the values of variables $(\nu_c, \chi_{c,k})$ in the n^{th} iteration. Similarly, the non-convex part of constraint (41a), i.e., the left-hand side is linearly approximated around the point $(\nu_k^{[n]}, \chi_{p,k}^{[n]})$ and the approximation is given by

$$\frac{\nu_k^2 a_{p,k}}{\chi_{p,k}} \geq a_{p,k} \left(\frac{2\nu_k^{[n]}}{\chi_{p,k}^{[n]}} \nu_k - \frac{(\nu_k^{[n]})^2}{(\chi_{p,k}^{[n]})^2} \chi_{p,k} \right) \triangleq \Psi_{p,k}^{[n]}(\nu_k, \chi_{p,k}). \quad (45)$$

Based on the approximations in (44) and (45), at iteration n problem (38) is approximated as,

$$\begin{aligned} & \max_{\substack{\boldsymbol{\nu}, \mathbf{c}, \boldsymbol{\alpha}_p, \boldsymbol{\alpha}_c, \\ \mathbf{r}_p, \mathbf{r}_c, \boldsymbol{\chi}_p, \boldsymbol{\chi}_c, t}} t \\ & \text{s.t. } \Psi_{c,k}^{[n]}(\nu_c, \chi_{c,k}) \geq r_{c,k} - 1, \forall k \in \mathcal{K}, \\ & \quad \Psi_{p,k}^{[n]}(\nu_k, \chi_{p,k}) \geq r_{p,k} - 1, \forall k \in \mathcal{K}, \\ & \quad (39b), (39c), (39d), (39e), (39h), \\ & \quad (40b), (41b), (42). \end{aligned} \quad (46)$$

Problem (46) is convex [37], which can be solved using standard convex optimization algorithms, i.e., interior-point methods. In the numerical results section, we make use of the CVX toolbox in Matlab to solve problem (46). Algorithm 3 outlines the SCA-based MaxMin power allocation algorithm of RS. In any iteration n , using the values $\boldsymbol{\nu}^{[n-1]}, \boldsymbol{\chi}_p^{[n-1]}, \boldsymbol{\chi}_c^{[n-1]}$ from the output of iteration $n-1$, problem (46) is solved and $t^{[n]}, \boldsymbol{\nu}^{[n]}, \boldsymbol{\chi}_p^{[n]}, \boldsymbol{\chi}_c^{[n]}$ are updated using the respective optimized values. The iterations continue till convergence is reached with a tolerance value ϵ .

Initialization: Since the variable $\boldsymbol{\nu}$ and auxiliary variables $\boldsymbol{\chi}_c$ and $\boldsymbol{\chi}_p$ all depend on $\boldsymbol{\rho}$, we begin with describing the initialization of $\boldsymbol{\rho}$. The initial power allocation is done by finding a feasible point $\boldsymbol{\rho}^{[0]}$

Algorithm 3 MaxMin: SCA Algorithm

- 1: **Initialize** $n \leftarrow 0$, $t^{[n]} \leftarrow 0$, $\nu^{[n]}$, $\chi_p^{[n]}$, $\chi_c^{[n]}$
 - 2: **Iterate**
 - 3: $n \leftarrow n + 1$;
 - 4: *Solve* (46) using $\nu^{[n-1]}$, $\chi_p^{[n-1]}$, $\chi_c^{[n-1]}$ and denote optimal values of t , ν , χ_p , χ_c as t^* , ν^* , χ_p^* , χ_c^* .
 - 5: **Update** $t^{[n]} \leftarrow t^*$, $\nu^{[n]} \leftarrow \nu^*$, $\chi_p^{[n]} \leftarrow \chi_p^*$, $\chi_c^{[n]} \leftarrow \chi_c^*$
 - 6: **Until** $|t^{[n]} - t^{[n-1]}| < \epsilon$
-

satisfying the transmit power constraint in (38c). With $\zeta \in [0, 1]$ denoting the fraction of total power allocated to the common stream, we have $\rho_c = \zeta \rho_{\text{dL}}$. Furthermore, $\rho_k = (1 - \zeta) \rho_{\text{dL}} / K$, $\forall k \in \mathcal{K}$ is the initial power allocated to each private stream. Consequently, $\nu_c^{[0]}$ and $\nu_k^{[0]}$ are respectively initialized as $\nu_c^{[0]} = \sqrt{\rho_c^{[0]}}$ and $\nu_k^{[0]} = \sqrt{\rho_k^{[0]}}$, $\forall k \in \mathcal{K}$, satisfying the transmit power constraint in (42). We initialize χ_c and χ_p by replacing the inequalities with equalities in (40b) and (41b), respectively.

Convergence: Since the constraints (40a) and (41a) are relaxed by the first-order lower bounds (44) and (45) respectively, a feasible solution of problem (46) at iteration n is also a feasible solution at iteration $n+1$. Therefore, the optimized value of t is always non-decreasing with n . As t is bounded by the transmit power constraint in (42), Algorithm 3 is guaranteed to converge. However, due to linear approximations (44) and (45), the algorithm is not guaranteed to converge to the global optimum. Initialization plays an important role in determining the optimized value of t and therefore, solving problem (46) for different values of ζ and selecting the optimal power allocation that maximizes t helps us achieve significantly better performance.

Remark. We would like to highlight that the SCA method is opted for MaxMin because of the joint optimization of power allocation coefficients and share of the common SE allocated to each UE in order to maximize the minimum SE. MaxSum-SE and MaxSINR power allocation problems can also be formulated and solved using the SCA method. However, we choose and illustrate Algorithm 1 for MaxSum-SE because different from MaxMin, MaxSum-SE only optimizes power allocation coefficients without the optimization of coupled common SE allocation. It is therefore possible to develop a power allocation strategy with a lower complexity and still achieve good SE performance. Since Algorithm 1 has a low time-complexity and builds on the popular uniform power allocation scheme of NoRS in practical networks, we choose Algorithm 1 to maximize the sum-SE of RS. For MaxSINR, we opt for Algorithm 2 because it provides the optimal solution to problem (35), as opposed to SCA which gives a sub-optimal solution. Nevertheless, Appendix B demonstrates the use of SCA algorithm to solve MaxSum-SE and MaxSINR problems of RS,

and their comparison with Algorithm 1 and Algorithm 2, respectively.

V. NUMERICAL RESULTS

To quantitatively compute the SE achieved by RS in TDD MaMIMO, we consider different topologies to capture different use cases and obtain the SE performance of RS and NoRS transmission strategies. For each topology, the SE results are obtained by averaging the SE over 100 setups. In each setup, the lower bound of the SE performance is calculated considering 200 coherence intervals. The two topologies considered in this paper are: 1) a rectangular topology where UEs are randomly distributed in a rectangular area of size $250 \times 250 \text{ m}^2$, illustrated in Fig. 3(a); and 2) a circular topology where UEs are randomly distributed around a circle of radius $r = 125 \text{ m}$, illustrated in Fig. 3(b). Here, both topologies are considered to appropriately capture use cases like conventional cellular use case, ultra-reliable low-latency communications (URLLC), mMTC and crowded scenarios.

At the transmitter side, the BS antennas are placed in a uniform linear array with half-wavelength antenna spacing. The large scale fading parameter path loss β_k for UE k is modelled in dB as [8, eq (2.3)]

$$\beta_k = \Gamma + 10\eta \log_{10}\left(\frac{d_k}{1\text{km}}\right) + S_k, \quad (47)$$

where d_k is the distance between the BS and UE k in km, the pathloss exponent η determines how fast the signal power decays and Γ is the channel gain at a distance 1 km. $S_k \in \mathcal{N}(0, \sigma_s^2)$ is the shadow fading coefficient. Subsequently, the corresponding channel correlation matrix for each UE is generated by assuming that each channel consists of $S = 10$ clusters following the Gaussian scattering model in [8, Sec 2.6]. Hence, the (m_1, m_2) th element of correlation matrix of UE k is given by

$$[\mathbf{R}_k]_{m_1, m_2} = \beta_k \times \frac{1}{S} \sum_{s=1}^S e^{i\pi(m_1 - m_2) \sin(\varphi_{k,s})} e^{-\frac{\sigma_\varphi^2}{2} (\pi(m_1 - m_2) \cos(\varphi_{k,s}))^2}. \quad (48)$$

Let φ_k be the geographical angle to UE k from the BS. Cluster s is characterized by a randomly generated nominal angle-of-arrival $\varphi_{k,s} \sim \mathcal{U}\{\varphi_k - 40^\circ, \varphi_k + 40^\circ\}$ and multipath components have their angles distributed around the corresponding nominal angle with variance $\sigma_\varphi = 15^\circ$. For uncorrelated Rayleigh fading, the spatial correlation matrix simply boils down to $\mathbf{R}_k = \beta_k \mathbf{I}_M$ [2]. The simulation parameters are reported in Table I.

We consider NoRS as the baseline strategy to compare the SE performance of RS. We choose MR precoding and calculate the SE performance of NoRS for all three different power allocation schemes as following

- *MaxSum-SE*: For MaxSum-SE, baseline NoRS results are obtained by switching off the common stream, i.e., by computing the sum-SE performance for $\zeta = 1$ in Algorithm 1.

Table I: Simulation parameters

Parameter	Value
Path Loss coefficients	$\Gamma = -148.1, \eta = 3.76, \sigma_s^2 = 16$
TDD parameters (samples)	$\tau = 200, \tau_p = 20, \tau_d = 190$
Total transmit powers	$\rho_{ul} = 10 \text{ dBm}, \rho_{dl} = 20 \text{ dBm}$
Noise powers	$\sigma_{ul}^2 = \sigma_n^2 = -94 \text{ dBm}$

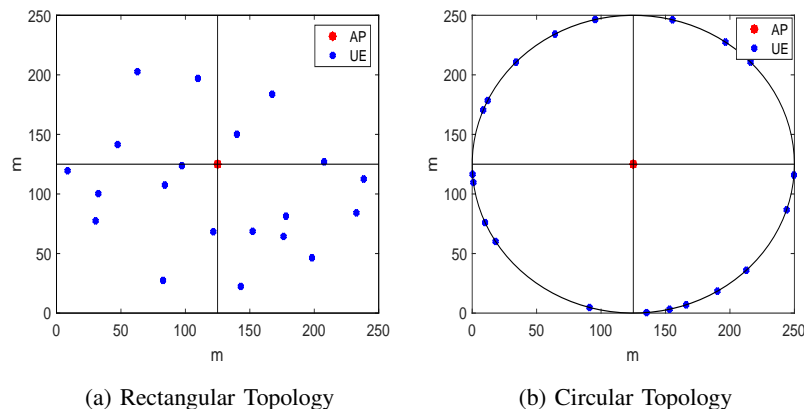


Figure 3: Network topologies.

- *MaxSINR*: MaxSINR problem of NoRS is formulated following equation (7.8) in [8]. MaxSINR problem with NoRS is also a GP problem and is solved using CVX.
- *MaxMin*: We opt for two Max-Min algorithms to obtain the SE performance of the NoRS strategy. In the first method, the common stream is switched off by allocating zero power to it, i.e., forcing $\rho_c = 0$, and then solving problem (46) using the SCA method. The second method is solving the MaxMin fairness problem (7.7) formulated in [8], which gives a globally optimal solution for a NoRS strategy by employing the Bisection algorithm. The first method (SCA) is considered to ensure fairness in MaxMin SE performance comparison of the RS and NoRS strategies, whereas the second method allows us to compare a sub-optimal SCA-based power allocation scheme of NoRS with the globally optimal algorithm of NoRS based on Bisection. The power allocation coefficients are initialized as $\rho_c = 0.1\rho_{dL}$ and $\rho_k = 0.9\rho_{dL}/K, \forall k \in \mathcal{K}$ for the MaxMin scheme of RS, whereas the initialization is $\rho_k = \rho_{dL}/K, \forall k \in \mathcal{K}$ for SCA-based MaxMin scheme of NoRS.

A. Orthogonal Pilots : No pilot contamination

We first illustrate the SE per UE of both RS and NoRS transmission strategies for the scenario when UL pilots are orthogonal to each other and user channels are spatially correlated. The SE per UE is obtained by employing the MaxMin power allocation scheme for both RS (Algorithm 3) and NoRS (SCA and

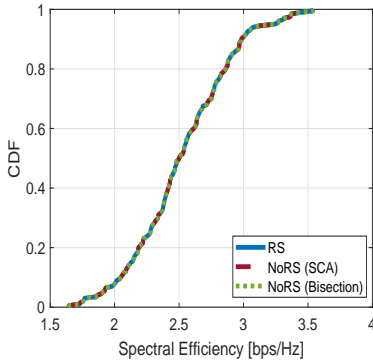


Figure 4: Average SE per UE, $M = 100$, $K = 8$, orthogonal pilots.

Bisection discussed in Section V) strategies. Fig. 4 illustrates the average SE per UE performance of both RS and NoRS strategies in the rectangular topology. We observe that since UEs use orthogonal pilots, there is no pilot contamination and both transmission strategies achieve high SE performance. Moreover, RS has no gain over NoRS. Note that since RS encapsulates a conventional linearly precoded multi-user MIMO strategy, under perfect CSI conditions, RS will always achieve a SE that is better than or equal to NoRS for the same optimization technique [39]. As a result, with perfect CSI, RS achieves the same SE performance as NoRS strategy, i.e. no power is allocated to the common streams and all the transmit power is allocated to the private streams. The SE result is similar for the circular topology and therefore is not illustrated for brevity. Moreover, the SE performance with spatially uncorrelated channel is consistent with the result of spatially correlated channels and is not shown to avoid redundancy.

B. Same Pilot: Severe pilot contamination

Next, we move to the other extreme and illustrate the SE per UE of both transmission strategies under severe pilot contamination for different topologies and propagation environments. The SE per UE results are obtained in the same way as in Section V-A. Fig. 5 illustrates the SE per UE performance of RS and NoRS strategy in the rectangular topology. From Fig. 5(a), we observe that the RS strategy is able to better manage the interference and achieves a better SE per UE performance than the NoRS strategy. Moreover, the gain of RS over NoRS is larger when the channel fading is uncorrelated. The reason is that while MMSE estimation is able to separate the channel estimates in the spatial domain when the UE channels are spatially correlated, it is unable to do the same with uncorrelated Rayleigh fading channels. As a result, the channel estimates get severely contaminated leading to a decrease in performance of both RS and NoRS strategy. However, due to the robustness of RS under imperfect CSI, the performance loss in RS is less severe compared to NoRS. Fig. 5(b) shows the average SE per UE versus the number of UEs

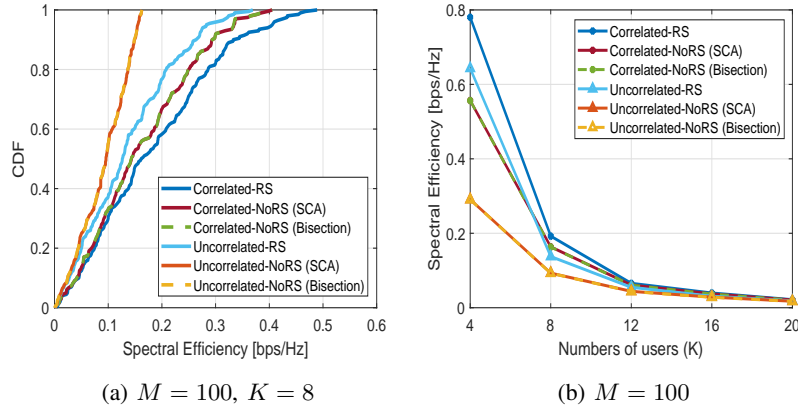


Figure 5: Average SE per UE in rectangular topology.

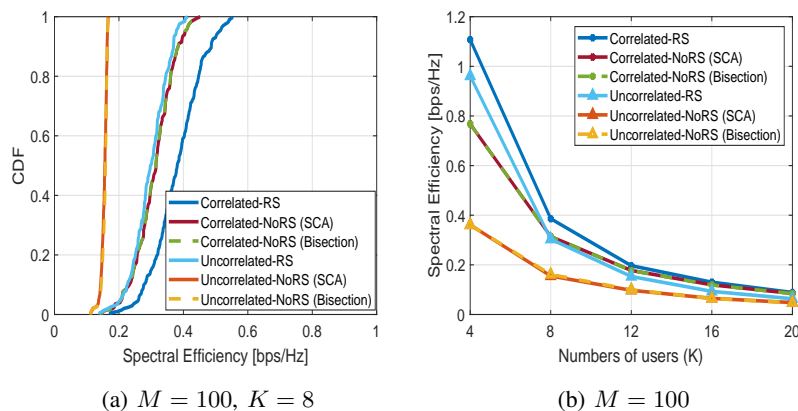


Figure 6: Average SE per UE in circular topology.

for the same network layout. For $K = 4$, the relative SE gain¹³ of RS over NoRS is 28.6% for correlated fading channels and 58.7% for uncorrelated fading channel. As the number of UE increases, both RS and NoRS show a sharp SE loss which can be attributed to multiple reasons. First, since all UEs are using the same pilot, the effect of pilot contamination becomes more severe as the number of UEs increases. Second, the objective of maximizing the minimum SE becomes more difficult as the number of UEs increases. For RS, the sharp decline also stems from the additional constraint of maximizing the common SE as the common stream is to be decoded by all UEs. Therefore, gain of RS over NoRS decreases as the number of UEs increases.¹⁴

Next we look at the performance of the transmission strategies in the circular topology. From Fig. 6, we observe that the gain of RS over NoRS is more explicit in the circular topology compared to the rectangular topology. This extra gain is due to the ease of the constraint of maximizing the common SE

¹³Relative SE gain is calculated as $\frac{SE^{RS} - SE^{NoRS}}{SE^{RS}}$.

¹⁴As the number of UEs increases, more advanced RS schemes could be used in MaMIMO to improve the performance [20], [33].

as UEs experience similar path loss. In this scenario, for $K = 4$, the gain of RS over NoRS is 30% for correlated fading channels and 62% for uncorrelated fading channels. Similarly, as observed in Fig. 6(b), the decline in average SE per UE is relatively less sharp in circular topology because equal path loss aids both maximizing the common SE and minimum total SE of a UE. As a result, the SE performance of RS is significantly higher than NoRS, even for a higher number of UEs. This is particularly beneficial for fixed mMTC scenarios where multiple active UEs (devices) have a high probability of sharing a pilot sequence and typically have low SE requirement in both UL and DL.

It should be highlighted that with spatially correlated channels, the relatively low gains of RS over NoRS for a higher number of UEs is not indicative of the true performance of RS. Since the UEs are randomly distributed within a area in rectangular topology, and along the circumference in circular topology, the channels of UEs are highly distinguishable in the spatial domain. In such a scenario, the MMSE estimation is better placed to separate the channel estimates in the spatial domain and even with a single pilot used for UL estimation, is better able to mitigate the effect of pilot contamination. However, if the UEs are packed within a sector, e.g. crowded scenarios, the efficacy of MMSE estimation in mitigating pilot contamination will suffer a SE loss. To elaborate, we compare the average SE per UE of RS and NoRS for the following two network layouts: 1) first, when the network layout is the same as Fig. 3, i.e., UEs are randomly distributed in the whole area of consideration ($\theta = 2\pi$) and 2) when UEs are randomly distributed within a confined sector ($\theta = \pi/4$), as illustrated in Fig. 7. It can be observed in Fig. 8(a) that though the achieved SE per UE decreases for both RS and NoRS as θ decreases to $\pi/4$ due to reduced CSI quality, the relative SE gain of RS over NoRS in rectangular topology increases from 15% to 23.5%. Similarly, the relative SE gain of RS over NoRS in circular topology illustrated in Fig. 8(b) increases from 18.6% to 35.33%. These results further attest the superiority of RS over NoRS strategy in different use cases by robustly managing interference and achieving high SE performance.

C. *MaxSum-SE and MaxSINR*

In this subsection, we illustrate the sum-SE performance of both RS and NoRS strategies with low complexity power allocation schemes which are more beneficial for use cases like mMTC. Taking note of the inferences from MaxMin results, we begin by focusing on the network layout with significant gains for RS, i.e., circular topology with UEs confined within a sector of $\theta = \pi/4$. From Fig. 9(a) and Fig. 9(b), we observe that for both power allocation schemes, the SE performance is consistent with the MaxMin power allocation scheme. While RS always achieves a higher sum-SE than NoRS, the gap is lower with spatially correlated channels. For $K = 8$, the SE gain of RS over NoRS with MaxSum-SE when UE channels are spatially correlated and uncorrelated is 20.9% and 42%, respectively. Moreover,

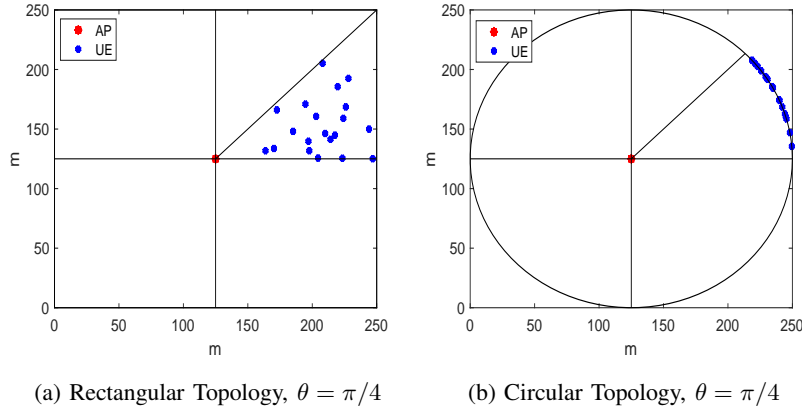


Figure 7: Network topologies with UEs confined within a sector.

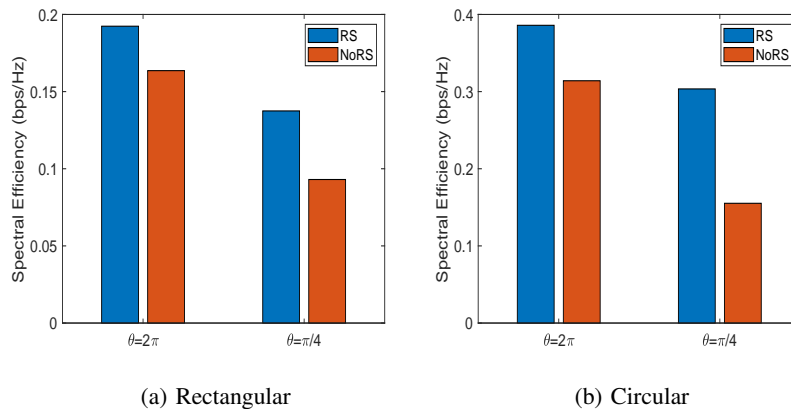


Figure 8: Average SE per UE with spatially correlated channels for different network layouts, $M = 100$ and $K = 8$.

both RS and NoRS achieve a lower sum-SE with MaxSINR compared to MaxSum-SE as number of UEs increases. This is because implicitly MaxSINR is designed to strike a balance between maximizing sum-SE and fairness. As a result, MaxSINR always allocates a non-zero power to each UE resulting in sum-SE performance loss. Note that, as observed with the MaxMin scheme, the gain of RS over NoRS decreases when the UEs are not confined to a sector and instead are randomly distributed over the entire circle. Similarly, the gap between the sum-SE of RS and NoRS will decrease in rectangular topology, i.e., when UEs experience different path loss. Nonetheless, even with low complexity power allocation schemes, RS is robust to imperfect CSI and achieves a better SE performance than NoRS.

D. Impact of number of transmit antennas

For the purpose of analysis, we continue with MaxSum-SE power allocation scheme and keep the network layout same as Fig. 7(b). Fig. 10(a) illustrates the sum-SE as a function of the number of transmit antennas, M , with the number of UEs $K = 8$. We observe that RS mitigates the effect of pilot

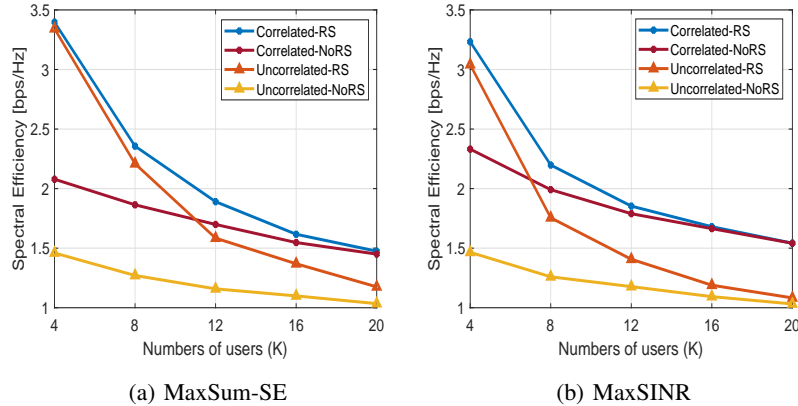


Figure 9: Sum-SE performance of the two low complexity power allocation schemes in circular topology, $M = 100$.

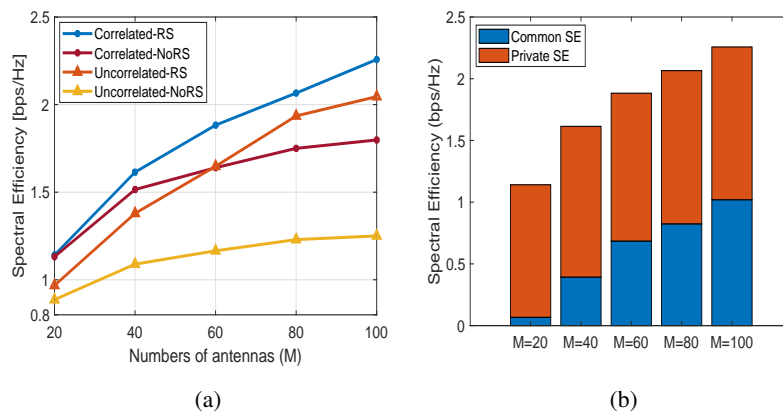


Figure 10: Sum-SE performance versus M , $K = 8$.

contamination even with a finite number of antennas and as M increases, the sum-SE gain of RS over NoRS increases. Since the effective propagation channel between the BS and UE k provides asymptotic channel hardening as $M \rightarrow \infty$, it aids in the SIC of the common stream. Therefore, as channel hardening increases, the performance gain of RS over NoRS increases due to better management of interference at the UE side. Note that the increase in the performance gain is more explicit with spatially uncorrelated channels than correlated channels. This behaviour can be attributed to the fact that spatial correlation undermines channel hardening in MaMIMO [40] thereby disallowing both RS and NoRS to exploit full potential of MaMIMO. Nonetheless, we observe from Fig. 10(b) that the contribution of common SE to the total sum-SE with spatially correlated channels increases from approximately 6% to 45% when M increases from 20 to 100. Therefore, the SE gain of RS over NoRS increases with the number of transmit antennas.

VI. CONCLUSION

In this paper, we proposed a general DL transmission framework of RSMA in TDD MaMIMO network. Based on the proposed framework, lower SE bounds for the common and private streams were derived that hold true for any choice of channel estimation and precoder design. Moreover, a low-complexity precoder design was formulated for the common stream of RS. We devised power allocation schemes for three different network utility functions such that the formulation holds for any choice of UL channel estimator and DL precoders. Considering both the ideal case when UEs use orthogonal pilots, and the worst case when multiple UEs share the same pilot in random access, we analyzed the SE performance of RS and NoRS. Through numerical simulations, we illustrated the SE performance of RSMA and compared it with that of a NoRS strategy in different network topologies and propagation environments. Numerical results showed that RSMA is significantly more robust to pilot contamination than NoRS transmission strategy.

Scarcity of pilots would be a major concern in B5G and 6G networks going forward, given their peculiar characteristics and use cases. Because of the adaptability and robustness of RSMA under different CSI regimes, RSMA would potentially play a significant role in MaMIMO networks. Building on the work done in this paper, future works could focus on studying multigroup multicasting in MaMIMO with RSMA and investigating RSMA as an inter-cell pilot contamination mitigation strategy. Furthermore, majority of the literature (including this paper) studying performance analysis of conventional TDD MaMIMO predominantly assumes the availability of channel statistics at the BS. The assumption allows for employing sophisticated signal processing algorithms like MMSE estimation to mitigate the effect of pilot contamination. However, in the absence of the knowledge of channel statistics, the difficulty of dealing with pilot contamination would increase significantly. Therefore, it would be interesting to study the potential benefits of RSMA under such constraints. Future works of RSMA in TDD MaMIMO could also focus on the interplay of RSMA with different UE grouping algorithms, UL performance of RSMA and performance of RSMA in TDD MaMIMO with DL training. Finally, other RS schemes, beyond the 1-layer RS architecture utilized here, could be leveraged to further enhance the performance.

APPENDIX A

We obtain the closed-form expression of the entity $\mathbb{E}\{\mathbf{h}_k^H \mathbf{w}_c^*\}$ as

$$\mathbb{E}\{\mathbf{g}_k^H \mathbf{w}_c^*\} = \frac{\sum_{i=1}^K a_i^* \text{tr}(\mathbf{R}_i \mathbf{Q}^{-1} \mathbf{R}_k)}{\sqrt{\sum_{i=1}^K \sum_{j=1}^K a_i^* a_j^* \text{tr}(\mathbf{R}_i \mathbf{Q}^{-1} \mathbf{R}_j)}}. \quad (49)$$

Similarly, the closed-form expression of $\mathbb{E}\{|\mathbf{g}_k^H \mathbf{w}_c^*|^2\}$ is obtained as

$$\mathbb{E}\{|\mathbf{g}_k^H \mathbf{w}_c^*|^2\} = \frac{\sum_{i=1}^K \sum_{j=1}^K a_i^* a_j^* \mathbb{E}\{\mathbf{g}_k^H \hat{\mathbf{g}}_i \hat{\mathbf{g}}_j^H \mathbf{g}_k\}}{\sum_{i=1}^K \sum_{j=1}^K a_i^* a_j^* \text{tr}(\mathbf{R}_i \mathbf{Q}^{-1} \mathbf{R}_j)}. \quad (50)$$

Using (3), numerator in equation (50) is reduced to

$$\begin{aligned}\mathbb{E}\{\mathbf{g}_k^H \widehat{\mathbf{g}}_i \widehat{\mathbf{g}}_j^H \mathbf{g}_k\} &= \mathbb{E}\{\mathbf{g}_k^H \widehat{\mathbf{g}}_i \widehat{\mathbf{g}}_i^H \mathbf{R}_i^{-1} \mathbf{R}_j \mathbf{g}_k\} \\ &= \text{tr}(\mathbf{R}_i^{-1} \mathbf{R}_j \mathbb{E}\{\mathbf{g}_k^H \widehat{\mathbf{g}}_i \widehat{\mathbf{g}}_i^H \mathbf{g}_k\}).\end{aligned}\quad (51)$$

As $\mathbf{g}_k = \widehat{\mathbf{g}}_k + \widetilde{\mathbf{g}}_k$, and $\widehat{\mathbf{g}}_k$ and estimation error $\widetilde{\mathbf{g}}_k$ are independent, (51) is further reduced to

$$\begin{aligned}\mathbb{E}\{\mathbf{g}_k^H \widehat{\mathbf{g}}_i \widehat{\mathbf{g}}_j^H \mathbf{g}_k\} &= \text{tr}(\mathbf{R}_i^{-1} \mathbf{R}_j \mathbb{E}\{\widehat{\mathbf{g}}_k^H \widehat{\mathbf{g}}_i \widehat{\mathbf{g}}_i^H \widehat{\mathbf{g}}_k\}) \\ &\quad + \text{tr}(\mathbf{R}_i^{-1} \mathbf{R}_j \mathbb{E}\{\widetilde{\mathbf{g}}_k \widetilde{\mathbf{g}}_k^H\} \mathbb{E}\{\widehat{\mathbf{g}}_i \widehat{\mathbf{g}}_i^H\}).\end{aligned}\quad (52)$$

Using equation (C.64) and equation (C.65) in [8], we get

$$\begin{aligned}\mathbb{E}\{\widehat{\mathbf{g}}_k^H \widehat{\mathbf{g}}_i \widehat{\mathbf{g}}_i^H \widehat{\mathbf{g}}_k\} &= \text{tr}(\Phi_i \Phi_k) + |\text{tr}(\mathbf{R}_i \mathbf{Q}^{-1} \mathbf{R}_k)|^2, \\ \mathbb{E}\{\widetilde{\mathbf{g}}_k \widetilde{\mathbf{g}}_k^H\} \mathbb{E}\{\widehat{\mathbf{g}}_i \widehat{\mathbf{g}}_i^H\} &= (\mathbf{R}_k - \Phi_k) \Phi_i,\end{aligned}\quad (53)$$

where \mathbf{R}_k and Φ_k are the correlation matrices of the channel and its estimate of UE k respectively. Substituting equation (53) into (52) and in turn substituting (52) into (50), closed-form expression for $\mathbb{E}\{|\mathbf{g}_k^H \mathbf{w}_c^*|^2\}$ is obtained.

APPENDIX B

A. MaxSum-SE: SCA

Similar to the problem (39), we introduce auxiliary variable α_c and vector $\boldsymbol{\alpha}_p = [\alpha_{p,1}, \dots, \alpha_{p,K}]$ representing the common SE and private SEs of UEs respectively. We introduce $\mathbf{r}_c = [r_{c,1}, \dots, r_{c,K}]$ and $\mathbf{r}_p = [r_{p,1}, \dots, r_{p,K}]$, representing 1 plus SINR value for common and private streams of UEs respectively and transform problem (34) equivalently as

$$\max_{\substack{\rho, \boldsymbol{\alpha}_p, \alpha_c, \\ \mathbf{r}_p, \mathbf{r}_c}} \alpha_c + \sum_{k=1}^K \alpha_{p,k}, \quad (54a)$$

$$s.t. \quad r_{p,k} - 2^{\frac{\tau}{\tau_d} \alpha_{p,k}} \geq 0 \quad \forall k \in \mathcal{K}, \quad (54b)$$

$$r_{c,k} - 2^{\frac{\tau}{\tau_d} \alpha_c} \geq 0 \quad \forall k \in \mathcal{K}, \quad (54c)$$

$$\frac{\rho_c a_{c,k}}{\sum_{i=1}^K \rho_i b_{ki}^c + \rho_c I_{c,k} + \sigma_n^2} \geq r_{c,k} - 1, \quad \forall k \in \mathcal{K}, \quad (54d)$$

$$\frac{\rho_k a_{p,k}}{\sum_{i=1}^K \rho_i b_{ki}^p + \rho_c I_{c,k} + \sigma_n^2} \geq r_{p,k} - 1, \quad \forall k \in \mathcal{K}, \quad (54e)$$

$$\alpha_c \geq 0, \quad (54f)$$

$$\rho_c + \sum_{i=1}^K \rho_i \leq \rho_{\text{dL}}. \quad (54g)$$

We can follow the SCA approach used to solve the MaxMin problem (39) and obtain the power allocation coefficients that aims to maximize the sum-SE.

Let us denote the SCA method utilized to maximize the sum-SE as “MaxSumSE-SCA”. Table II compares the SCA method and Algorithm 1 in terms of the CPU time consumed to obtain the sum-SE performance with a single pilot used by $K = 4$ UEs for uplink training. We observe that MaxSumSE-SCA achieves 30.7% higher sum-SE performance but the time taken increases approximately 10^5 fold. The reason for the stark difference in time taken by the two methods is that Algorithm 1 considers a linear one dimensional exhaustive search of ζ between 0 and 1 to maximize the sum-SE, whereas MaxSumSE-SCA is an iterative method that aims to maximize the sum-SE. Note that, the time consumed and sum-SE performance of MaxSumSE-SCA also depend on the power allocation initialization. For comparison in Table II, we initialize the power allocation coefficients as $\rho_c = 0.1\rho_{\text{dL}}$ and $\rho_k = 0.9\rho_{\text{dL}}/K, \forall k \in \mathcal{K}$.

Table II: MaxSum-SE: Performance Comparison

	Algorithm 1	SCA
CPU time (secs)	0.0013	86.94
SE (bps/Hz)	3.47	5.01

B. MaxSINR: SCA

We introduce auxiliary variable α_c and auxiliary vector $\boldsymbol{\alpha}_p = [\alpha_{p,1}, \dots, \alpha_{p,K}]$ representing the log of common SINR and private SINRs of UEs respectively. Similarly, we introduce $\mathbf{r}_c = [r_{c,1}, \dots, r_{c,K}]$ and $\mathbf{r}_p = [r_{p,1}, \dots, r_{p,K}]$, representing SINR value for common and private streams of UEs respectively and transform problem (35) equivalently as

$$\max_{\rho, \boldsymbol{\alpha}_p, \alpha_c, \mathbf{r}_p, \mathbf{r}_c} \alpha_c + \sum_{k=1}^K \alpha_{p,k}, \quad (55a)$$

$$s.t. \quad r_{p,k} - 2^{\alpha_{p,k}} \geq 0 \quad \forall k \in \mathcal{K}, \quad (55b)$$

$$r_{c,k} - 2^{\alpha_c} \geq 0 \quad \forall k \in \mathcal{K}, \quad (55c)$$

$$\frac{\rho_c a_{c,k}}{\sum_{i=1}^K \rho_i b_{ki}^c + \rho_c I_{c,k} + \sigma_n^2} \geq r_{c,k}, \quad \forall k \in \mathcal{K}, \quad (55d)$$

$$\frac{\rho_k a_{p,k}}{\sum_{i=1}^K \rho_i b_{ki}^p + \rho_c I_{c,k} + \sigma_n^2} \geq r_{p,k}, \quad \forall k \in \mathcal{K}, \quad (55e)$$

$$\alpha_c \geq 0, \quad (55f)$$

$$\rho_c + \sum_{i=1}^K \rho_i \leq \rho_{\text{dL}}. \quad (55g)$$

Let us denote the SCA method utilized to maximize the product of SINRs as “MaxSINR-SCA”. Compared to Algorithm 2, MaxSINR-SCA achieves approximately 20% lower sum-SE performance and consumes 8 fold more time. Specific form of the objective and constraints, and modern solvers allows Algorithm 2

based on GP to efficiently optimize the power coefficients and find an optimal solution in significantly less time [41]. As a result, Algorithm 2 outperforms MaxSINR-SCA in terms of both SE and time consumed to obtain the sum-SE. For MaxSINR-SCA as well, the time and sum-SE performance depend on the initialization of the power coefficients, which are as in Appendix B-A.

Table III: MaxSINR: Performance Comparison

	Algorithm 2	SCA
CPU time (secs)	4.33	34.10
SE (bps/Hz)	3.24	2.62

REFERENCES

- [1] C. K. Thomas *et al.*, “A rate splitting strategy for mitigating intra-cell pilot contamination in massive MIMO,” in *IEEE Int. Conf. Commun. (ICC) Workshop*, 2020, pp. 1–6.
- [2] L. Sanguinetti *et al.*, “Toward Massive MIMO 2.0: Understanding spatial correlation, interference suppression, and pilot contamination,” *IEEE Trans. Commun.*, vol. 68, no. 1, pp. 232–257, 2020.
- [3] E. Björnson *et al.*, “Massive MIMO has unlimited capacity,” *IEEE Trans. Wireless Commun.*, vol. 17, no. 1, pp. 574–590, 2018.
- [4] E. Björnson, L. Sanguinetti, H. Wymeersch, J. Hoydis, and T. Marzetta, “Massive MIMO is a reality—What is next?” *Digital Signal Processing*, vol. 94, 06 2019.
- [5] T. L. Marzetta, “Massive MIMO: An introduction,” *Bell Labs Technical Journal*, vol. 20, pp. 11–22, 2015.
- [6] E. G. Larsson *et al.*, “Massive MIMO for next generation wireless systems,” *IEEE Commun. Mag.*, vol. 52, no. 2, pp. 186–195, 2014.
- [7] E. Björnson *et al.*, “Massive MIMO: ten myths and one critical question,” *IEEE Commun. Mag.*, vol. 54, no. 2, pp. 114–123, 2016.
- [8] E. Björnson, J. Hoydis, and L. Sanguinetti, “Massive MIMO networks: Spectral, energy, and hardware efficiency,” *Foundations and Trends® in Signal Processing*, vol. 11, no. 3-4, pp. 154–655, 2017.
- [9] J. Jose *et al.*, “Pilot contamination problem in multi-cell TDD systems,” in *IEEE Int. Symp. Inf. Theory*, 2009, pp. 2184–2188.
- [10] E. Björnson and E. G. Larsson, “Three practical aspects of massive MIMO: Intermittent user activity, pilot synchronism, and asymmetric deployment,” in *2015 IEEE Globecom Workshops (GC Wkshps)*, 2015, pp. 1–6.
- [11] J. H. Sørensen *et al.*, “Massive MIMO for crowd scenarios: A solution based on random access,” in *2014 IEEE Globecom Workshops (GC Wkshps)*, 2014, pp. 352–357.
- [12] E. de Carvalho *et al.*, “Random access for massive MIMO systems with intra-cell pilot contamination,” in *IEEE Int. Conf. Acoust., Speech, Signal Process. (ICASSP)*, 2016, pp. 3361–3365.
- [13] A. Mishra, Y. Mao, L. Sanguinetti, and B. Clerckx, “Rate-splitting assisted massive machine-type communications in cell-free massive MIMO,” *IEEE Commun. Lett.*, pp. 1–1, 2022.
- [14] D. Neumann *et al.*, “Suppression of pilot-contamination in massive MIMO systems,” in *IEEE 15th Int. Workshop Signal Process. Adv. Wireless Commun. (SPAWC)*, 2014, pp. 11–15.
- [15] T. X. Vu *et al.*, “Successive pilot contamination elimination in multiantenna multicell networks,” *IEEE Wireless Commun. Lett.*, vol. 3, no. 6, pp. 617–620, 2014.
- [16] K. Appaiah *et al.*, “Pilot contamination reduction in multi-user TDD systems,” in *IEEE Int. Conf. Commun. (ICC)*, 2010, pp. 1–5.
- [17] V. Saxena *et al.*, “Mitigating pilot contamination by pilot reuse and power control schemes for massive MIMO systems,” in *IEEE 81st Veh. Techno. Conf. (VTC2015-Spring)*, 2015, pp. 1–6.
- [18] K. Upadhyaya *et al.*, “Superimposed pilots are superior for mitigating pilot contamination in massive MIMO,” *IEEE Trans. Signal Process.*, vol. 65, no. 11, pp. 2917–2932, 2017.

- [19] W. A. W. M. Mahyiddin *et al.*, “Pilot contamination reduction using time-shifted pilots in finite massive MIMO systems,” in *IEEE 80th Veh. Techno. Conf. (VTC2014-Fall)*, 2014, pp. 1–5.
- [20] Y. Mao, B. Clerckx, and V. O. K. Li, “Rate-splitting multiple access for downlink communication systems: bridging, generalizing, and outperforming SDMA and NOMA,” *EURASIP J. Wireless Commun. Netw.*, vol. 2018, no. 1, p. 133, May 2018.
- [21] A. Mishra *et al.*, “Rate-splitting multiple access for 6G—Part I: Principles, applications and future works,” *arXiv preprint:2205.02548*, 2022.
- [22] O. Dizdar *et al.*, “Rate-splitting multiple access: A new frontier for the PHY layer of 6G,” in *IEEE 92nd Veh. Techno. Conf. (VTC2020-Fall)*, 2020, pp. 1–7.
- [23] Y. Mao *et al.*, “Rate-splitting multiple access: Fundamentals, survey, and future research trends,” *arXiv preprint: 2201.03192*, 2022.
- [24] B. Clerckx *et al.*, “Rate splitting for MIMO wireless networks: A promising PHY-layer strategy for LTE evolution,” *IEEE Commun. Mag.*, vol. 54, no. 5, pp. 98–105, May 2016.
- [25] A. Mishra *et al.*, “Rate-splitting multiple access for downlink multiuser MIMO: Precoder optimization and PHY-layer design,” *IEEE Trans. Commun.*, pp. 1–1, 2021.
- [26] C. Hao *et al.*, “Achievable DoF regions of MIMO networks with imperfect CSIT,” *IEEE Trans. Inf. Theory*, vol. 63, no. 10, pp. 6587–6606, Oct. 2017.
- [27] A. Gholami Davoodi and S. Jafar, “Degrees of Freedom region of the (M, N_1, N_2) MIMO broadcast channel with partial CSIT: An application of sum-set inequalities based on aligned image sets,” *IEEE Trans. Inf. Theory*, vol. 66, no. 10, pp. 6256–6279, 2020.
- [28] H. Joudeh and B. Clerckx, “Sum-rate maximization for linearly precoded downlink multiuser MISO systems with partial CSIT: A rate-splitting approach,” *IEEE Trans. Commun.*, vol. 64, no. 11, pp. 4847–4861, Nov. 2016.
- [29] E. Piovano and B. Clerckx, “Optimal DoF region of the K-user MISO BC with partial CSIT,” *IEEE Commun. Lett.*, vol. 21, no. 11, pp. 2368–2371, Nov. 2017.
- [30] Y. Mao, B. Clerckx, and V. O. K. Li, “Energy efficiency of rate-splitting multiple access, and performance benefits over SDMA and NOMA,” in *Proc. IEEE Int. Symp. Wireless Commun. Syst. (ISWCS)*, Aug. 2018, pp. 1–5.
- [31] H. Joudeh and B. Clerckx, “Robust transmission in downlink multiuser MISO systems: A rate-splitting approach,” *IEEE Trans. Signal Process.*, vol. 64, no. 23, pp. 6227–6242, Dec. 2016.
- [32] Y. Mao and B. Clerckx, “Beyond dirty paper coding for multi-antenna broadcast channel with partial CSIT: A rate-splitting approach,” *IEEE Trans. Commun.*, vol. 68, no. 11, pp. 6775–6791, 2020.
- [33] M. Dai *et al.*, “A rate splitting strategy for massive MIMO with imperfect CSIT,” *IEEE Trans. Wireless Commun.*, vol. 15, no. 7, pp. 4611–4624, July 2016.
- [34] A. Papazafeiropoulos *et al.*, “Rate-splitting to mitigate residual transceiver hardware impairments in massive MIMO systems,” *IEEE Trans. Veh. Technol.*, vol. 66, no. 9, pp. 8196–8211, 2017.
- [35] H. Yin *et al.*, “Dealing with interference in distributed large-scale MIMO systems: A statistical approach,” *IEEE J. Sel. Topics Signal Process.*, vol. 8, no. 5, pp. 942–953, 2014.
- [36] H. Q. Ngo and E. G. Larsson, “No downlink pilots are needed in TDD massive MIMO,” *IEEE Trans. Wireless Commun.*, vol. 16, no. 5, pp. 2921–2935, 2017.
- [37] S. Boyd and L. Vandenberghe, “Convex Optimization,” in *Cambridge, U.K.: Cambridge Univ. Press*, 2004.
- [38] Y. Mao *et al.*, “this paper fairness of k-user cooperative rate-splitting in MISO broadcast channel with user relaying,” *IEEE Trans. Wireless Commun.*, vol. 19, no. 10, pp. 6362–6376, 2020.
- [39] B. Clerckx *et al.*, “Is NOMA efficient in multi-antenna networks? a critical look at next generation multiple access techniques,” *IEEE Open J. Commun. Soc.*, vol. 2, pp. 1310–1343, 2021.
- [40] J. Nam *et al.*, “Capacity scaling of massive MIMO in strong spatial correlation regimes,” *IEEE Trans. Inf. Theory*, vol. 66, no. 5, pp. 3040–3064, 2020.
- [41] W. Hoburg and P. Abbeel, “Geometric programming for aircraft design optimization,” *AIAA Journal*, vol. 52, no. 11, pp. 2414–2426, 2014.